Proceedings of the ASME 2010 3rd Joint US-European Fluids Engineering Summer Meeting and
8th International Conference on Nanochannels, Microchannels, and Minichannels
FEDSM-ICNMM2010
August 1-5, 2010, Montreal, Canada

FEDSM-ICNMM2010-31220

EX-SITU CHARACTERIZATION OF TWO-PHASE FLOW REGIMES IN PROTON-EXCHANGE MEMBRANE FUEL CELLS UNDER NON-ISOTHERMAL CONDITIONS.

Arganthaël Berson
Fuel Cell Research Centre – Queen's University
Kingston, Ontario, Canada

Jon G. Pharoah
Fuel Cell Research Centre – Queen's University
Kingston, Ontario, Canada

ABSTRACT

Efficient water management is crucial for the good performances of proton-exchange membrane fuel cells (PEMFCs). The geometric and physical characteristics of the components of a PEMFC as well as operating conditions have an impact on the transport of water through the porous transport layer (PTL) and the two-phase flow regimes in the micro-channels. One parameter of importance is the local temperature, which affects properties such as surface tension and is coupled with phase change. Indeed, a temperature difference of about 5K is expected across the PTL, with spatial variations due to the geometry of the flow field plate.

We present preliminary results obtained with a first experimental setup for the ex-situ characterization of two-phase flow regimes in the flow channels. Water is pushed through the PTL, which is sandwiched between a porous metal foam and the flow field plate. The air flow rate, temperature and humidity can be controlled. The cell can be heated up by applying an electrical current through the metal foam. A transparent window is located on top of the flow channel. The two-phase flow within the micro-channels is visualized using a high-speed camera and laser-induced fluorescence. Preliminary results obtained under isothermal conditions at room temperature show that different two-phase flow regimes occur in the channels depending on the operating conditions, in good qualitative agreement with data from the literature.

Eventually, a new visualization cell is presented that is expected to correct the flaws of the previous design and will allow a better thermal control. It will be possible to adjust the temperature gradient and the mean temperature in order to observe their impact on two-phase flow regimes for different types of PTL and flow rates. The results will provide a better understanding of water transport in PEMFC and benchmark data for the validation of numerical models.

INTRODUCTION

Efficient water management is a necessity in order to achieve high-performance Proton-Exchange Membrane Fuel Cells (PEMFC). For optimal operation, the membrane needs to be properly hydrated. However, too high water content might hinder the supply of reactants to the reaction sites and decrease the performances. Water is generated at the cathode as a result of the oxygen reduction reaction. Excess liquid water is mainly removed through the Porous Transport Layer (PTL, a.k.a. gas diffusion layer) and the micro-channels where it is washed away by the flow of reactants.

The flow of water through the PTL is dominated by fingering and channeling due to the operating conditions and the finite size of the PTL (e.g. [1-5]). There are preferential water pathways through the PTL that lead to preferential locations where droplets emerge. The dynamics of water transport in the PTL have been explored by Bazylak et al. [3]. They showed that when more preferable pathways inside the PTL appear, less preferable ones recede so that preferential breakthrough locations may vary with time. Such behavior has been observed experimentally by Ous et Arcomanis [6]. It suggests an eruptive process of evacuation of water to the channels, which was confirmed by recent high-resolution synchrotron X-ray radiography experiments [7, 8]. These experiments also clearly demonstrate that water transport is a dynamic process.

Water transport inside the PTL and the emergence of water in the channels depend on operating conditions such as current density (e.g [9-13]), the type of PTLs (e.g. [9, 13]) and their compression by the flow field plate, which favors the accumulation of water under the lands (e.g. [11, 13, 14]). The operating temperature also affects the liquid water content of a PEMFC [12, 15, 16, 17]. High operating temperatures (≈80°C) favor evaporation. Indeed, experimental evidence [15, 17] and non-isothermal mathematical models [17-20] show that temperature affects phase change, which in turns has an impact on water transport. The temperature in the gas channels is lower than the temperature at the membrane electrode interface. The temperature difference across the PTL is of the order of about 5K at a current density of $1A/cm^2$ [18, 21]. In [17] and [20], it was suggested that the temperature gradient across the PTL creates a "heat-pipe effect" or "phase-change-induced flow"', i.e. evaporation drives the transport of water vapor down the temperature gradient, from the MEA to the flow channels. The removal of water in the vapor phase is of course more efficient than it is in the liquid phase, which is beneficial for the performances of the PEMFC. However, the water-vapor flux goes against the transport of reactants to the catalyst layer. In addition, the increased generation of water vapor decreases the partial pressure of reactants. Both these effects are detrimental since they limit the current.

Operating conditions also affect two-phase flow regimes in the channels. At high air flow rate, droplets emerging from the PTL are readily removed by the air flow and a mist flow regime is observed [6, 22-25] whereas, at low air flow rate, drag forces are not sufficient to detach the droplets that stay pinned to the PTL [6, 23-25]. Then, water removal is ensured either by coalescence with droplets coming from upstream, either by migration of water along the more hydrophilic walls of the channel. Film flows were reported by several studies including [22-25]. Note that if the film grows thick enough, it may become unstable and block the channel [25]. Film flow may occur also at high airflow velocity when droplets touch a side wall while emerging [22]. Droplets touching a side wall may also remain attached and grow continuously as water is extracted from the PTL so that they can block the channel [6, 22]. Hussaini et Wang [24] proposed to categorize the different flow regimes observed in the micro-channels onto a flow map.

Our objective is to investigate the effect on two-phase flow in the channels of various parameters such as the mass flow rate and temperature of air and water, air humidity, the properties of the flow channels and the PTL, the operating temperature and the temperature gradient across the PTL. In order to vary these parameters independently, a visualization cell mimicking an actual fuel cell has been built. First, we present the experimental setup. Second, we show preliminary results obtained under isothermal conditions at room temperature. Eventually, a new design of the visualization cell is presented.

EXPERIMENTAL SETUP

Visualization cell

A schematic view of the visualization cell is given in Figure 1. The base of the visualization cell consists of a water reservoir in which plates of porous metal foam (Recemat Ni-Cr foam) are inserted. The role of the porous metal foam is to create a homogeneous distribution of water at the interface with the PTL while providing mechanical support. In addition, we can apply an electrical current through the metal foam with the help of a current generator connected to two electrodes on the sides of the metal foam plates. The current heats up the cell by Joule effect up to a desired operating temperature controlled by a thermocouple inserted between the metal foam and the PTL.

The PTL is sandwiched between the metal foam and the flow field plate. On top of the cell, a transparent acrylic window provides an optical access for the visualization. The different parts are assembled in a press and tightened with 10 screws at a torque of 100lb.in in order to ensure a compression of the cell as even as possible.

The design of the setup allows to change the flow field plates and the PTLs in order to investigate their effect on water transport. In the following, we used a flow field plate made of aluminum (contact angle ≈ 90°). It consists of 5 parallel serpentine channels. Each channel has a square cross section of 1mm x 1mm. The active surface area is 10cm x 10cm. The PTL corresponding to the results presented in the following sections is a SGL 31 BC, with 5% PTFE and an MPL.

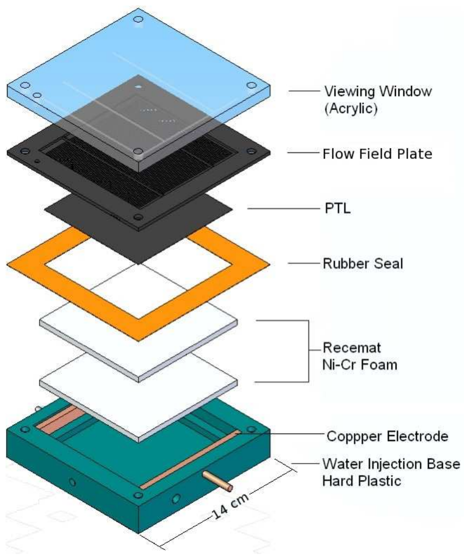

Figure 1 - Schematic drawing of the visualization cell. Exploded view.

Control system

The experimental setup is schematized in Figure 2. The air flow rate is imposed by a mass flow controller (MKS 5000 sccm) located between a bottle of compressed air and an Arbin humidifier system, which controls air humidity and temperature. The tubes carrying humidified air to the cell are maintained at a constant temperature in order to prevent condensation of water on the way to the cell. Water is heated to the desired operating temperature in a water bath and injected into the base with the help of a Gilson 307 HPLC pump. The pressure inside the water reservoir is controlled with a pressure sensor (Omega PX603). As mentioned previously, the cell is heated up by passing an electrical current through the porous metal foam. The temperature is monitored by a thermocouple located between the metal foam and the PTL.

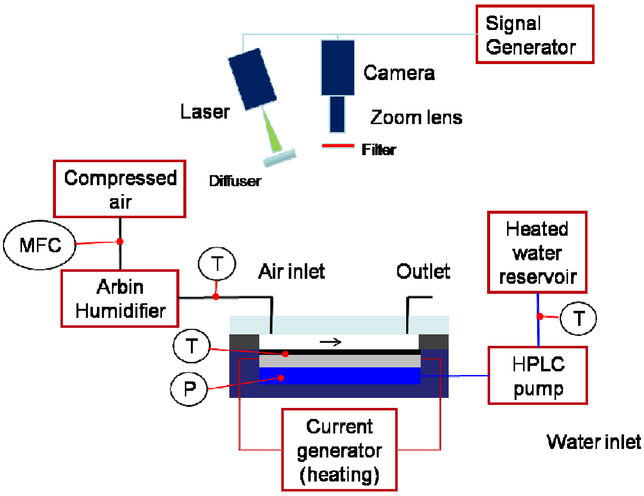

Figure 2 - Schematics of the experimental setup. MFC indicates a mass flow controller, T indicates thermocouples and P indicates a pressure sensor.

Imaging system

Images were taken with a high-speed digital camera Red Lake IDT M5 (up to 170fps at full resolution). The camera is mounted with a Fujinon 35-mm lens. The measurement area is approximately 10cm x 12cm. Illumination is performed by a Nd:YAG double-pulse laser (NewWave Solo) with a wavelength of 532nm (green). The laser is connected to a fiber optics. The laser beam comes at an angle with respect to the camera axis and a diffuser is used to provide an even illumination of the measurement area. The camera and the laser are synchronized together based on a periodic signal generated by a signal generator.

In order to improve the quality of the images, a fluorescent dye (Rhodamine B) is added to water. The fluorescent dye re-emits light at a wavelength of 625nm (orange) when excited by the laser. An optical filter is added in front of the lens so that only the frequencies corresponding to the dyed water are transmitted to the camera. Therefore, interfaces between liquid water and the gas flow in the channels are clearly distinguishable.

In order to enhance the contrast and improve the quality of the measurements, the images are post-processed. First, a background image taken before liquid water started to appear the channels is subtracted to the raw images. Then, images are reduced to a zone of interest, converted into grayscale and the contrast is intensified.

PRELIMINARY RESULTS

First measurements were performed under isothermal conditions at room temperature (22°C) with no heating of the cell, air or water. Different operating conditions were tested:

- Case 1: m_{H2O}=0.5mL/min and m_{air}=3000mL/min, which corresponds to a current density of I=0.9A/cm^2 and a stoichiometry of λ=2.
- Case 2: m_{H2O}=0.5mL/min and m_{air}=2000mL/min, which corresponds to a current density of I=0.9A/cm^2 and a stoichiometry of λ=1.2.
- Case 3: m_{H2O}=0.5mL/min and m_{air}=500mL/min, which corresponds to a current density of I=0.9A/cm^2 and a stoichiometry of λ=0.35.

Images of the two-phase flow observed in the channels for the different cases are presented in Figure 3. The different cases yield different two-phase flow regimes. At high air flow rate (case 1) only traces of liquid water are observed in the channel. As the air flow rate decreases (case 2), a film flow is observed. Water is found along the walls while air flows in the center of the channel. Eventually, at low air flow rate (case 3), water plugs appear that clog the channel.

These results are in good qualitative agreement with data from the literature obtained in transparent fuel cells (e.g. [24]) However, further work is necessary in order to validate the repeatability of the measurements, to create flow maps that relate the different flow regimes to operating conditions and to assess the effect of various parameters including the type of PTL, thermal effects, location along the channels and PTL compression on the two-phase flow regimes.

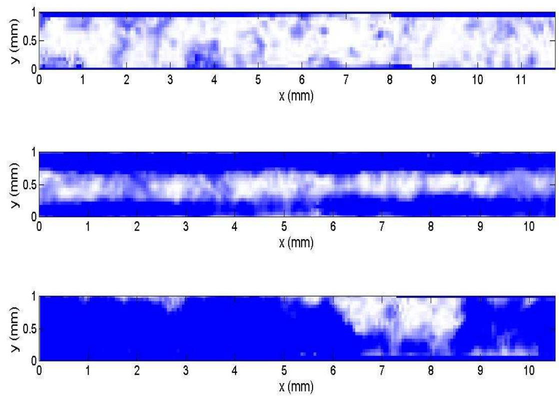

Figure 3 - Visualization of liquid water in the channels. Top: single-phase flow observed for case 1. Middle: film flow observed for case 2. Bottom: slug flow observed for case 3. High levels of blue indicate the presence of liquid water.

NEW VISUALIZATION CELL

The preliminary results presented in the previous section allowed us to demonstrate the feasibility of our experimental setup. However, several flaws in the design of the visualization cell including leaks, difficulties to control the temperature near the PTL or uncontrolled temperature at the top of the flow channels led us to design a new cell that is presented in Figure 4.

The new design is expected to correct the flaws of the previous one. First, the measurement area has been reduced to a 1-inch-diameter disc, which yields a more homogeneous compression of the PTL. We also improved the sealing.

Second, the new design is expected to provide a better control of temperature distributions in the cell. A thermal buffer including a water circulation loop is added on top of the visualization window. The water circulation imposes a constant temperature to the cell, e.g. 80°C. This part also acts as a thermal buffer so that the window on top of the channels can be made of regular acrylic (contact angle ≈70°, which is close to the contact angle of regular graphite bipolar plates) without being subject to condensation on its surface. On the contrary, the top window, which is not in contact with the flow channels, is made of surface-treated anti-fog acrylic in order to prevent condensation. At the bottom of the cell, the water reservoir and the perforated plate on which the PTL is located are made of copper, which is a good heat conductor. Cartridge heaters are inserted in the water reservoir. The role of the heaters is not to heat the entire cell but rather to create a temperature gradient across the PTL, similar to what is observed in operating fuel cells. The temperature gradient across the PTL will be monitored by thermocouples located on both sides of the PTL. Preliminary estimates using COMSOL 3.5 show that 100W cartridge heaters will be sufficient to generate a 5K gradient across the PTL. Tests are underway to verify that the desired temperature distributions can be achieved in the new setup. In addition, pressure measurements in the water reservoir and the flow channels will allow to monitor the evolution of the capillary pressure with the buildup of water within the PTL.

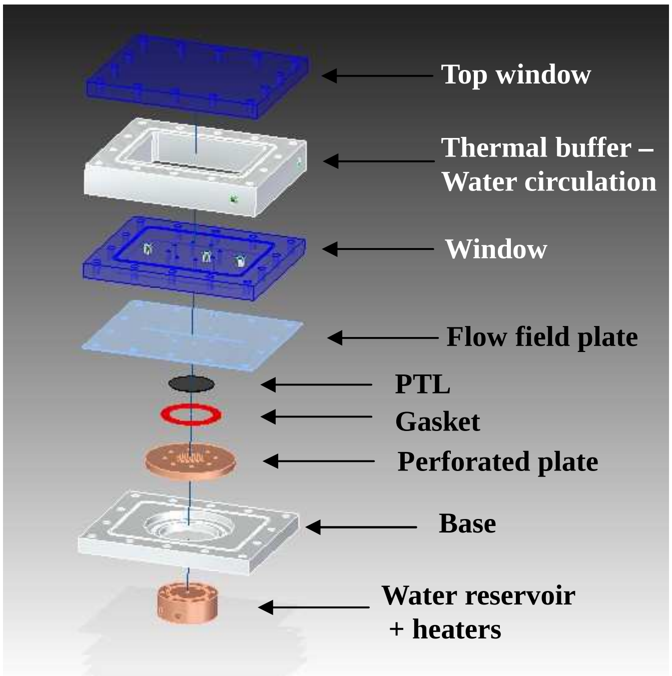

Figure 4 - Schematic drawing of the new visualization cell - Exploded view.

CONCLUSIONS

We designed a visualization cell for the ex-situ investigation of the effect of various operating conditions, including temperature, on the two-phase flow regimes inside the flow channels of a PEMFC. Results obtained with a first experimental setup under isothermal conditions at room temperature are in good qualitative agreement with previous observations reported in the literature. At low air flow rate, slug flow was observed in the channels, where liquid water forms plugs that clog the channel. As the air flow rate increases, film flow was observed. At high air flow rate no significant amount of liquid water was observed in the channels.

These results are encouraging and demonstrate the feasibility of our project. However, we had to build a new visualization cell in order to correct several problems in the original design. We hope to present results obtained with the new setup in the final version of the paper and during the conference.

ACKNOWLEDGMENTS

The authors acknowledge Matthew Schuster who designed the first visualization cell described in the paper.

REFERENCES

1. Bazylak A., Sinton D., Liu Z.S., Djilali N. (2007), Effect of compression on liquid water transport and microstructure of PEMFC gas diffusion layers, Journal of Power Sources, 163, pp.784-792.
2. Litster S., Sinton D., Djilali N. (2006), Ex situ visualization of liquid water transport in PEM fuel cell gas diffusion layers, Journal of Power Sources, 154, pp.95-105.
3. Bazylak A., Sinton D., Djilali N. (2008), Dynamic water transport and droplet emergence in PEMFC gas diffusion layers, Journal of Power Sources, 176, pp.240-246.
4. Rebai M., Prat M. (2009), Scale effect and two-phase flow in a thin hydrophobic porous layer. Application to water transport in gas diffusion layers of proton exchange membrane fuel cells, Journal of Power Sources, 192(2), pp.534-543.
5. Sinha P.K., Mukherjee P.P., Wang C.Y. (2007), Impact of GDL structure and wettability on water management in polymer electrolyte fuel cells, J. Mater. Chem., 17, pp.3089-3103.
6. Ous T., Arcoumanis C. (2007), Visualisation of water droplets during the operation of PEM fuel cells, Journal of Power Sources, 173, pp.137-148.
7. Manke I., Hartnig Ch., Gr¨unerbel, Lehnert W., Kardjilov N., Haibel A., Hilger A., Banhart J., Riesemeier H. (2007), Investigation of water evolution and transport in fuel cells with high resolution synchrotron x-ray radiography, Applied Physics Letters, 90, 174105.

8. Hartnig Ch., Manke I., Kuhn R., Kleinau S., Goebbels J., Banhart J. (2009), High-resolution in-plane investigation of the water evolution and transport in PEM fuel cells, Journal of Power Sources, 188, pp.468-474.

9. Ito K., Ashikaga K., Masuda H., Oshima T. (2008), Estimation of flooding in PEMFC gas diffusion layer by differential pressure measurement, Journal of Power Sources, 175, pp.732-738.

10. Kramer D., Zhang J., Shimoi R., Lehmann E., Wokaun A., Shinohara K., Scherer G.G. (2005), In situ diagnostic of two-phase flow phenomena in polymer electrolyte fuel cells by neutron imaging Part A. Experimental, data treatment, and quantification, Electrochimica Acta, 50, pp.2603-2614.

11. Owejan J.P., Trabold T.A., Jacobson D.L., Arif M., Kandlikar S.G. (2007), Effects of flow field and diffusion layer properties on water accumulation in a PEM fuel cell, International Journal of Hydrogen Energy, 32, pp.4489-4502.

12. Park J., Li X., Tran D., Abdel-Baset T., Hussey D.S., Jacobson D.L., Arif M. (2008), Neutron imaging investigation of liquid water distribution in and the performance of a PEM fuel cell, International Journal of Hydrogen Energy, 33, pp.3373-3384.

13. Zhang J., Kramer D., Shimoi R., Ono Y., Lehmann E., Wokaun A., Shinohara K., Scherer G.G. (2006), In situ diagnostic of two-phase flow phenomena in polymer electrolyte fuel cells by neutron imaging Part B. Material variations, Electrochimica Acta, 51, pp.2715-2727.

14. Bazylak A., Sinton D., Liu Z.S., Djilali N. (2007), Effect of compression on liquid water transport and microstructure of PEMFC gas diffusion layers, Journal of Power Sources, 163, pp.784-792.

15. Hickner M.A., Siegel N.P., Chen K.S., Hussey D.S., Jacobson D.L., Arif M. (2008), In situ high-resolution neutron radiography of cross-sectional liquid water profiles in proton exchange membrane fuel cells, J. Electrochem. Soc. 155(4), pp.B427-B434.

16. Ous T., Arcoumanis C. (2009), Visualisation of water accumulation in the flow channels of PEMFC under various operating conditions, Journal of Power Sources, 187, pp.182-189.

17. Kim S., Mench M.M. (2009), Investigation of temperature-driven water transport in polymer electrolyte fuel cell: Phase-change-induced flow, J. Electrochem. Soc., 156(3), pp.B353-B362.

18. Weber A.Z., Newman J. (2006), Coupled thermal and water management in polymer electrolyte fuel cells, J. Electrochem. Soc., 153(12), pp.A2205-2214.

19. Wang Y., Wang C.Y. (2006), A nonisothermal, two-phase model for polymer electrolyte fuel cells, J. Electrochem. Soc., 153(6), pp.A1193-A1200.

20. Weber A.Z., Hickner M.A. (2008), Modeling and high-resolution-imaging studies of water-content profiles in a polymer-electrolyte-fuel-cell membrane electrode assembly, Electrochimica Acta, 53, pp.7668-7674.

21. Vie P.J.S., Kjelstrup S. (2004), Thermal conductivities from temperature profiles in the polymer electrolyte fuel cell, Electrochimica Acta, 49, pp.1069-1077.

22. Spernjak D., Prasad A.K., Advani S.G. (2007), Experimental investigation of liquid water formation and transport in a transparent single-serpentine PEM fuel cell, Journal of Power Sources, 170, pp.334-344.

23. Zhang F.Y., Yang X.G., Wang C.Y. (2006), Liquid water removal from a polymer electrolyte fuel cell, Journal of the Electrochemical Society, 153(2), pp.A225-A232.

24. Hussaini I.S.,Wang C.-Y. (2009), Visualization and quantification of cathode channel flooding in PEM fuel cells, Journal of Power Sources, 187, pp.444-451.

25. Yang X.G., Zhang F.Y., Lubawy A.L., Wang C.Y. (2004), Visualization of liquid water transport in a PEFC, Electrochemical and Solid-State Letters, 7(11), pp.A408-A411.